IOP Conf. Series: Materials Science and Engineering **256** (2017) 012013 doi:10.1088/1757-899X/256/1/012013

High-speed precise cell patterning by pulsed electrohydrodynamic jet printing

A V Makaev*, E A Mingaliev, V R Karpov, I V Zubarev, V Ya Shur, and O S El'kina

Ural Federal University, Ekaterinburg, 620002, Russia

*makaev.andrew@yandex.ru

Abstract. The generation of micro-droplets of nutrient medium with living cells by pulsed electrohydrodynamic printing has been studied. In-situ visualization by high-speed camera made it possible to measure the characteristic times of droplet generation process and to determine the optimal printing parameters. Maximal frequency of stable generation was achieved at 700 Hz. This technique was applied successfully for drop-on-demand printing of culture medium with live HeLa cells and yeasts.

1. Introduction

Electrohydrodynamic (EHD) printing is a method of generating a droplet or a continuous jet by the application of an electric field to drop meniscus [1]. Among many direct writing methods, EHD printing has much potential for high resolution patterning [2]. EHD printing is driven by a strong electric field generated by a voltage between the nozzle with charged liquid and a grounded electrode [3, 4]. The essential diminishing of the droplet size as compared with the nozzle diameter allows producing micron-scale droplets without tube contamination [5].

Compatibility with different materials, applicability for large substrates, high targeting accuracy, relative simplicity, and non-vacuum and non-contact approach makes EHD printing attractive and suitable to wide range of applications. Moreover, the big viability (above 95%) [6] of cells subjected to EHD deposition on the substrate initiated its application in cellular and tissue engineering for the manipulation and placement of various cells on culture plates and scaffolds [7, 8].

Recently, in order to demonstrate drop-on-demand printing in the cone-jet mode, many researchers have adapted a square voltage pulse superposed by a dc bias voltage [9-13]. The short high-voltage pulse releases a droplet (or a finite number of droplets) from the nozzle, while the lower bias needs to ensure that a near conical shaped meniscus is always present, but not discharging any fluid [12, 13]. Therefore, the jetting start time can be shortened and the jetting frequency can be maximized [14, 15]. After termination of the rectangular voltage pulse, the meniscus may oscillate and recede back to the initial position through oscillation damping time [14]. Consequently, for a stable drop-on-demand jetting, the next pulse should be applied after the oscillation damping time. Besides, the meniscus oscillation may generate the unwanted secondary droplets. Therefore, to maximize drop-on-demand jetting frequency, it would be helpful to study the dynamics of the meniscus oscillation.

In this paper, we have demonstrated essential improvement of the main characteristics of EHD printing method using bias voltage with opposite sign to pulse voltage for minimizing the oscillation amplitude and the damping time. This technique was applied successfully for drop-on-demand printing of culture medium with live HeLa cells and yeasts.

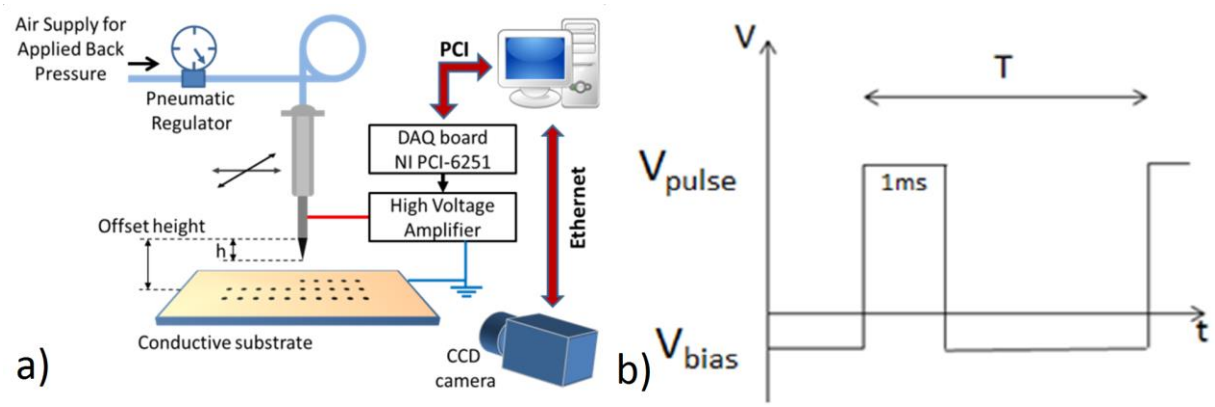

Figure 1. (a) Scheme of experimental setup for the droplet generation. (b) Waveform of applied voltage.

2. Experimental

The experimental setup consisted of a solution chamber fixed on three-axial translation stage, high-voltage power supply, and conductive substrate (Fig. 1a). The solution passed through a metal nozzle (inner diameter: 280 μm, outer diameter: 420 μm) at a constant flow rate controlled by air supply, which applied back pressure (≤ 5 psi) using pneumatic pressure controller (9THE-200, Taeha Corporation). The droplet generation was stimulated by the rectangular high voltage pulses (Fig. 1b) applied between the needle and glass substrate using the high-speed high-voltage power amplifier (Trek-10/10B-HS, TREK Inc.). The glass substrate was covered by 300-nm-thick Ti layer. The pulse amplitude below 2.5 kV and the current below 0.1 mA were used to prevent unwanted corona discharge and to ensure almost pure electrostatic force generation. Pulse duration equal to 1 ms was chosen to generate one droplet per pulse. The high speed CCD camera (Photron FASTCAM Mini UX100) with frame rate up to 10000 fps was used for in situ recording of the droplet generation and meniscus oscillation.

Multifunctional Cartesian robot with programmable motion controller (JC-3A00-0H3, Janome Sewing Machine CO. LTD.) was used for relocation and exact positioning of the solution camera in X-Y-Z directions. Such system allows depositing droplets according to the designed patterns. The arrays of dispensing droplets were visualized by optical microscope (Olympus BX-61) and scanning electron microscope (Auriga CrossBeam, Carl Zeiss).

Two types of solutions were used: (1) gelatin water solution and (2) DMEM medium. For gelatin solution, 50 mL of distilled water, 1 g of yeasts, and 1g of gelatin were added and the mixture was stirred for 30 min at 40°C. The solutions were kept at room temperature during 20 min and then were subjected to electrohydrodynamic printing. The HeLa cells were obtained from Institute of Immunology and Physiology UB RAS in Ekaterinburg. The cells were cultured in high-glucose Dulbecco's modified Eagle medium (H-DMEM; Invitrogen) with 10% fetal bovine serum (FBS; Hyclone) in a CO_2 incubator at 37°C and with 5% CO_2. The Hela cells were subcultured by trypsin (0.25%, invitrogen) dissociation at about 80% confluences.

3. Results and discussion

3.1. Visualization of droplet generation

EHD drop-on-demand printing exploits the high voltage pulses applied between the metal nozzle with liquid and the ground electrode, which induces charge accumulation at the liquid meniscus, forcing the meniscus to become more convex (i.e., increase the surface tension pressure) for balancing the electric pressure. The meniscus becomes conical and emits a fluid jet, when the electric pressure exceeds the surface tension pressure. In case of drop-on-demand printing, the constant V_{bias} forms near conical shaped meniscus, whereas the short-range V_{pulse} leads to jet emission. As noted above, the serious problem of printing is instability caused by oscillation of liquid meniscus after pulse voltage

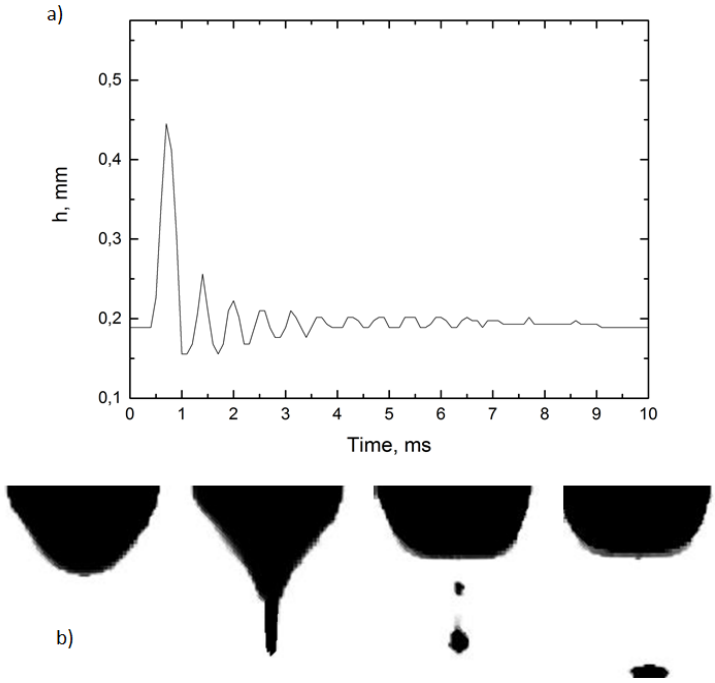

Figure 2. (a) The time dependence of the meniscus apex height *h* during droplet generation. (b) Main stages of the DMEM droplet generation.

termination leading to decrease of droplet generation frequency, and dripping of undesirable secondary droplets. The high-speed *in-situ* visualization of droplet meniscus behavior during generation process was carried out. The sequence of instantaneous images of drop meniscus is presented in Figure 2b.

The following main stages of the droplet generation were distinguished: (1) the deformation of the drop meniscus in the short-lived Taylor cone, (2) the emission of transient jet, (3) the dripping of a droplet, and (4) the damped oscillations of the meniscus. To characterize quantitatively the droplet generation process, the time dependence of the meniscus apex height *h* was extracted by specially developed software (Fig. 2a).

3.2. Generation of droplets at different bias voltages

To investigate the influence of V_{bias} magnitude on the damped oscillations, the time dependence of the meniscus apex height at different V_{bias} was calculated. The chosen V_{pulse} = 2.5 kV is slightly less than

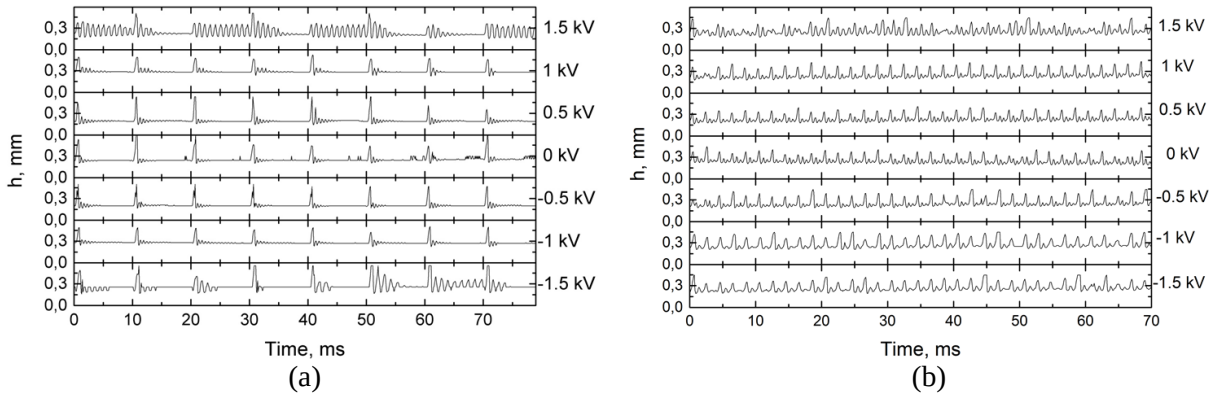

Figure 3. The time dependences of the cone apex height for pulse series with different V_{bias} for frequency: (a) 100 Hz, (b) 700 Hz.

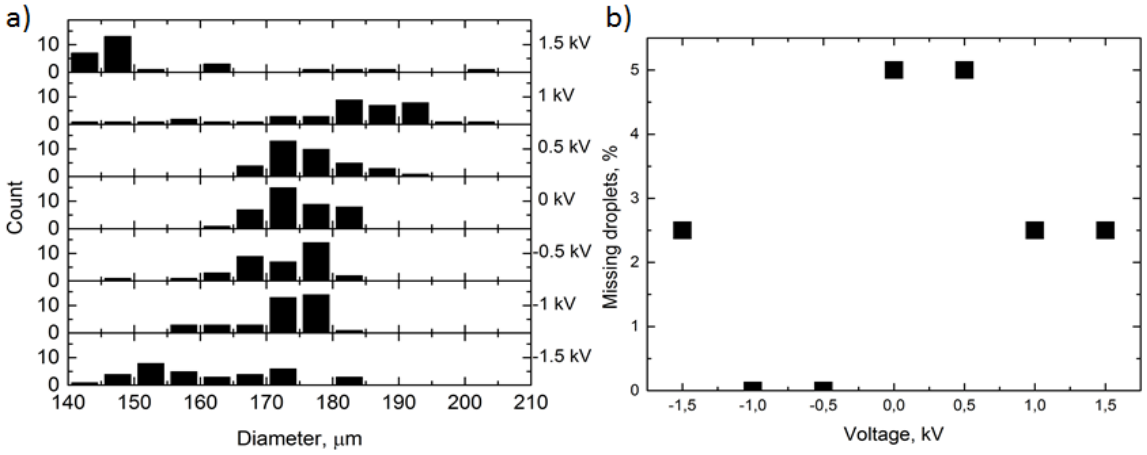

Figure 4. (a) Histogram of droplet diameter. (b) Percent of missing droplets in array.

the breakdown voltage leading to voltaic arc between nozzle and substrate. V_{bias} was varied between 1,5 kV and -1,5 kV at offset height of nozzle above the substrate 500 μm. Frequency of the pulse voltage generation was 100 Hz for nozzle translation speed v = 50 mm/s.

The jetting start time (time interval between the rising edge of the voltage pulse and the jet emission) was about 0.4 ms for all V_{bias}. The duration of transient jet existence was less than time resolution of the method, which was 0.1 ms. However, the duration of the damped oscillations exceeded several milliseconds and depended significantly on the sign and the value of V_{bias} (Fig. 3).

It was obtained that at high V_{bias} (+1.5 kV) the oscillation dumping time was comparable with pulse period (10 ms), being a consequence of the large amplitude of the oscillations after pulse termination (Fig. 3a). Moreover, we observed non-reproductive and unstable generation process – different lengths of transient jets and appearance of repeated jets in the interval between pulses leading to generation of unwanted secondary droplets. As a result, the droplets obtained at high V_{bias} have the wide range of diameters (Fig. 4a). It should be noted that there are 2.5% missing droplets in the array (Fig. 4b).

Decreasing of V_{bias} leads to reduction of both oscillation amplitude and damping time. As a result, the quantity of secondary droplets was reduced, but the missing droplets in the array were also present.

Then, we investigated the droplet generation using negative V_{bias}. As we can see in Figure 4, at V_{bias} = -1 kV and -0.5 kV the small variance of diameters and absence of missing droplets have been obtained. This can be explained by the braking force created by the counteracting electrical pressure, which effectively suppresses the meniscus oscillations after the pulse termination. Hence, shot oscillation dumping time and nonzero V_{bias} lead to the fact that at the beginning of the next voltage pulse the meniscus will take a conic shape with the apex in the previous position. Also, at these parameters the secondary droplets were not observed due to small amplitude of oscillations. At the same time, the dispensing accuracy (mean distance between center of droplets and programmed place) was slightly better (5.3 μm) than that for the best result obtained at the positive V_{bias} (8.8 μm).

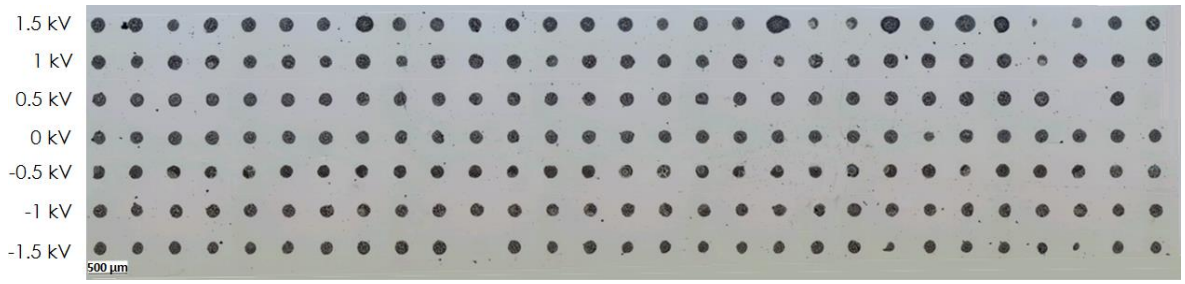

Figure 5. Optical images of linear arrays of DMEM droplets printed at different V_{bias}. V_{pulse} = 2.5 kV, f = 100 Hz, v = 50 mm/s.

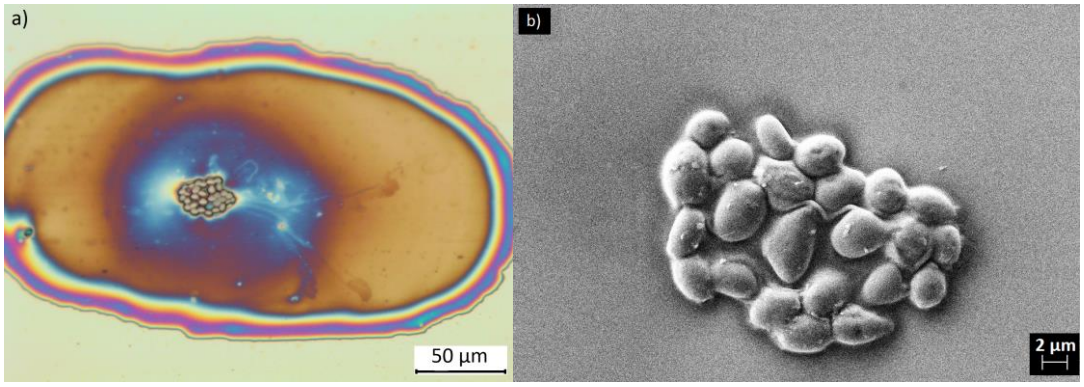

Figure 6. Gelatine droplets with few tens of yeast cells printed on glass substrate covered by 300-nm-thick Ti layer: (a) optical image, (b) scanning electron microscopy image.

Further increasing of negative V_{bias} worsened the results. As seen in Figure 3a, at V_{bias} = -1.5 kV continuous chaotic oscillations were observed. Electric pressure was too high at both directions and meniscus drop oscillations did not dump sometimes, being similar to behavior at V_{bias} = 1.5 kV (Fig.5).

At frequency of generation f = 700 Hz with nozzle translation speed v = 100 mm/s the difference in meniscus oscillations at various V_{bias} became smaller, but, nevertheless, small negative V_{bias} demonstrated the best accuracy and entirety of droplets array.

Summarizing, at high bias voltages (1.5 kV and -1.5 kV) we get unstable droplet generation with missing and secondary droplets. At lower bias voltages, we get rid of secondary droplets and dispensing droplets are obtained with small variance of diameters. But, at positive and zero voltages, percent of missing droplets in array increased. The best results without secondary and missing droplets and with narrow distribution of droplet diameter were obtained for generation at low negative V_{bias}. So, for suppressing meniscus oscillations we proposed to use negative voltage as a baseline voltage. For stable generation, it is necessary to ensure that a near conical shaped meniscus is always present, but not discharging any fluids. Therefore, negative voltage solves both problems – suppresses oscillations of meniscus and holds meniscus in the near conical shaped form.

3.3. Printing by living cells

This technique was used to realize drop-on-demand printing by culture medium with live cells. The regular arrays of gelatin solution droplets with yeast cells were printed on glass substrate covered with 300-nm-thick Ti layer in Figure 6. The few tens of cells were located in the center of each gelatine droplet in the region with diameter below 50 µm. Viability of yeasts was tested with trypan blue and was more than 95%.

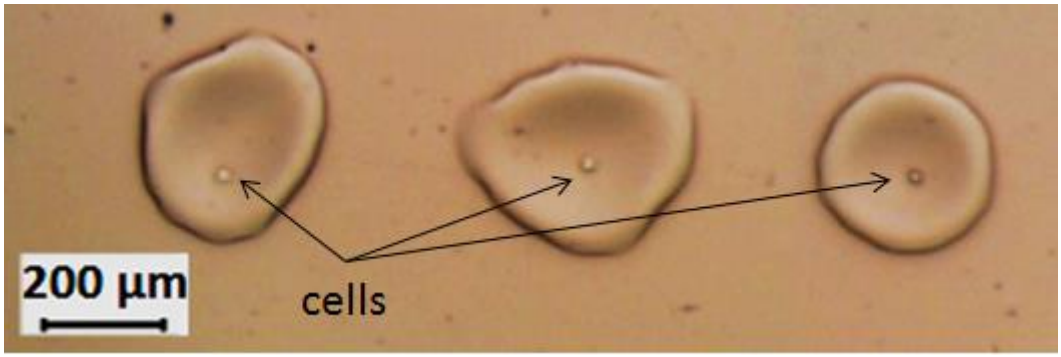

Figure 7. Droplets of Dulbecco's modified Eagle medium with HeLa cells.

The arrays of DMEM medium droplets with few HeLa cells (Fig. 7) in each were printed on the glass substrate covered with gelatin thin layer. The existence of the layer of gelatine, which was needed to prevent fast evaporation of the cultural medium, led to non-reproducibility of droplet sizes due to the ineffective screening of the induced static charges.

4. Conclusions

The high-speed droplet dispensing was achieved using electrohydrodynamic technique. Process of droplet dispensing was visualized with time resolution 0.1 ms and the main stages of droplet generation were distinguished. The measurement of the characteristic times of droplet generation process allowed defining parameters of voltage pulses for stable printing process and achieving maximum frequency of generation 700 Hz. The method was applied successfully for printing by culture medium with living cells: DMEM culture with HeLa cells and yeasts cell in gelatin water solution.

Acknowledgments

The research was carried out using the equipment of Ural Center for Shared Use "Modern Nanotechnologies" UrFU, with the financial support of the Government of the Russian Federation (Act 211, Agreement 02.A03.21.0006) and Ministry of Education and Science of the Russian Federation (Project No. 3.9534.2017/BP).

References

[1] Collins R T, Jones J J, Harris M T and Basaran O 2008 *Nat. Phys*. **4** 149–54
[2] Park J-U, Hardy M, Kang S J, Barton K, Adair K, Mukhopadhyay D K, Lee C Y, Strano M S, Alleyne A G, Georgiadis J G, Ferreira P M and Rogers J 2007 *Nat. Mater*. **6** 782–9
[3] Onses M S, Sutanto E, Ferreira P M, Alleyne A G and Rogers J A 2015 *Small* **11** 4237–66
[4] Taylor G 1964 *Proc. R. Soc. A Math. Phys. Eng. Sci* **280** 383–97
[5] Chen C H, Seville D A and Aksay I A 2006 *Appl. Phys. Lett* **89** 124103
[6] Zhao X, He J, Xu F, Liu Y and Li D 2016 *Virtual. Phys. Prototyp* **11** 57–63
[7] Gudapati H, Dey M and Ozbolat I 2016 *Biomaterials* **102** 20–42
[8] Murphy S V and Atala A 2014 *Nat. Biotechnol*. **32** 773–85
[9] Tran S B Q, Byun D, Nguyen V D and Kang T S 2009 *Phys. Rev.* E **80** 1–11
[10] Kwon K-S and Lee D-Y 2013 *J. Micromech. Microeng.* **23** 65018
[11] Kim J, Oh H and Kim S S 2008 *J. Aerosol Sci*. **39** 819–25
[12] Mishra S, Barton K L, Alleyne G, Ferreira P M and Rogers J 2010 *J. Micromech. Microeng.* **20** 95026
[13] Lee S, Song J, Kim H and Chung J 2012 *J. Aerosol Sci.*, vol. **52**, pp. 89–97
[14] Yang J, Kim H, Cho B and Chung J 2014 *J. Mech. Sci. Technol*. **28** 2815–23
[15] Li J L 2007 *J. Electrostat.* **65** 750–7